Journal of Applied Physics ARTICLE scitation.org/journal/jap

The Cu photoluminescence defect and the early stages of Cu precipitation in Si

Cite as: J. Appl. Phys. **127**, 085704 (2020); doi: 10.1063/1.5140456
Submitted: 2 December 2019 · Accepted: 6 February 2020 ·
Published Online: 25 February 2020

T. M. Vincent,[1] S. K. Estreicher,[1,a)] J. Weber,[2] V. Kolkovsky,[2] and N. Yarykin[3]

AFFILIATIONS

[1]Physics Department, Texas Tech University, Lubbock, Texas 79409-1051, USA
[2]Institut für Angewandte Physik, Technische Universität Dresden, 01062 Dresden, Germany
[3]Institute of Microelectronics Technology RAS, Chernogolovka 142432, Russia

Note: This paper is part of the Special Topic on Defects in Semiconductors 2020.
[a)]**Author to whom correspondence should be addressed:** stefan.estreicher@ttu.edu

ABSTRACT

This theoretical–experimental study focuses on the formation of the substitutional-tri-interstitial cluster $Cu_{s1}Cu_{i3}$, which has been proposed as the photoluminescence defect Cu_{PL}. The configurations and electronic properties of the intermediate defects $Cu_{s1}Cu_{i1}$ and $Cu_{s1}Cu_{i2}$ are calculated, and their electrically active levels are obtained from conventional and Laplace deep-level transient spectroscopy. The vacancy formation energy near copper-related defects is calculated and found to be much smaller than in the perfect crystal. Then, we show how $Cu_{s1}Cu_{i3}$ could become the seed of agglomerates of $Cu_{s1}Cu_{i3}$ "units." The discussion focuses mostly on unanswered questions about the discrepancies between the calculated and measured properties of Cu_{PL} and $Cu_{s1}Cu_{i3}$.

I. INTRODUCTION

A. Copper in silicon

Copper is a common contaminant in Si devices and solar cells.[1] Sources of Cu are the chemicals used during device processing, the metallic contacts, and the slurries used for polishing. Isolated Cu is almost entirely interstitial, usually in the +1 charge state (Cu_i^+). It is one of the fastest-diffusing impurities in Si with a migration barrier of 0.18 eV.[2–4] Cu_i^+ behaves as a small closed-shell $3d^{10}4sp^0$ ion with very little chemical activity. A level detected at $E_c - 0.15$ eV was associated with its donor state.[5]

A fraction of the copper finds a pre-existing vacancy (V_{Si}, the concentration depends on the history of the sample) and forms electrically active substitutional copper (Cu_s) with a calculated energy gain of about 3.13 eV.[6] Here, copper promotes some electron density from the 3d to the 4sp shell in order to optimize the covalent interactions with its four Si nearest neighbors (NNs). Thus, the strength of each Cu–Si bond is about 0.78 eV. Cu_s has a calculated[6] (measured[7–10]) donor level at $E_v + 0.20$ eV ($E_v + 0.20$–0.23), acceptor level at $E_c - 0.72$ eV ($E_v + 0.42$–0.48), and a double-acceptor level at $E_c - 0.16$ eV ($E_c - 0.16$). Therefore, in low to moderately doped samples, Cu_i is Cu_i^+ while Cu_s is in 0 or −1 charge state, depending on the temperature, doping, and Cu_i concentration (which can move the Fermi level in p-type Si). It is believed that rapidly diffusing Cu_i^+s trap at Cu_s leading to the Cu_{PL} photoluminescence (PL) center.[6,11,12]

When Cu is introduced into Si, it readily precipitates at dislocations, grain boundaries, oxygen precipitates, internal voids, and other extended defects.[13–15] When Cu is introduced into defect-free Si at high temperatures and the sample cools down, it quickly becomes supersaturated. In p-type Si, most of it is Cu_i^+, and the Coulomb repulsion prevents internal precipitation. Cu then outdiffuses to the surface.[16] In n-type Si, Cu forms electrically active silicides,[16–18] but their nucleation process is not known.

B. The Cu_{PL} defect

The low-temperature PL band with a zero-phonon line at 1014 meV and sharp phonon sidebands at 7.05 meV was first reported by Minaev *et al.*[19] and shown to be Cu-related by Weber *et al.*[20] Uniaxial stress and Zeeman data of the zero-phonon line show that the center is trigonal.[20] All the available data are consistent with the model of a pseudo-donor.[20,21] The Cu_{PL} defect has been correlated with a donor level at $E_v + 0.10$ eV.[22] The thermal

dissociation of the Cu_{PL} center was reported to be about 1.6 eV, and the dissociation takes place in about 2 h at 200 °C.[8] The much lower dissociation energies of about 0.5 and 1.0 eV[23–25] could be the results of unintentional H contamination, an impurity known[26] to enhance the annealing of Cu_{PL}.

After annealing of the Cu_{PL} defect, only Cu_s remains, showing that Cu_s is the core of Cu_{PL}.[7,8,27,28] For many years, this center was commonly believed to be a substitutional–interstitial Cu_sCu_i pair,[20] and theoretical studies confirmed that this pair has indeed the key features of Cu_{PL}.[29] However, PL studies in isotopically pure ^{28}Si samples[30,31] have produced much sharper lines where individual Cu isotopes can be clearly identified. These experiments have shown that Cu_{PL} contains (at least) four Cu atoms. No two-Cu or three-Cu defects could be identified in the PL spectra.

Shirai *et al.*[11] proposed a trigonal defect consisting of one substitutional and three interstitial copper atoms ($Cu_{s1}Cu_{i3}$) but did not calculate the gap levels nor propose an explanation as to why the 2-Cu or 3-Cu defect is not seen. A more comprehensive theoretical study by Carvalho *et al.*[6] has shown that the formation energy of the trigonal $Cu_{s1}Cu_{i3}$ defect is the lowest of all 4-Cu clusters for all positions of the Fermi level. If the Fermi level is about midgap, the calculated defect levels assign the −1 charge state to Cu_s, $Cu_{s1}Cu_{i1}$, and $Cu_{s1}Cu_{i2}$, while $Cu_{s1}Cu_{i3}$ remains electrically neutral. The Coulomb attraction with Cu_i^+ would enhance the formation of successive $Cu_{s1}Cu_{in}$ clusters up to n = 3. However, experiments show that Cu_{PL} forms in p-type Si as well.[8,22]

The binding energies of all three Cu_i components in the $Cu_{s1}Cu_{i3}$ model were calculated[6] to be about the same and below 1 eV. However, experiments show a higher binding energy for the Cu_{PL} center. Further, the calculated donor level of the $Cu_{s1}Cu_{i3}$ complex[6,32] is much higher in the gap than the observed $E_v + 0.10$ eV.

C. Scope of this contribution

In the present study, we perform a theoretical study of $Cu_{s1}Cu_{in}$ (with n = 1–4). The binding energies and the gap levels are predicted, including the double-donor and double-acceptor levels. Conventional deep-level transient spectroscopy (DLTS) and Laplace DLTS (LDLTS) measurements show the presence of several new levels in the gap, which are compared with the calculated ones.

We then focus on how this center could become the building block of larger Cu precipitates. Following studies in specially prepared Si samples, Ohno *et al.*[33] proposed coherent structures made from $Cu_{s1}Cu_{i3}$ building blocks. This raises the question of how a single $Cu_{s1}Cu_{i3}$ grows into larger complexes. The key is that the formation energy of V_{Si} strongly depends on where V_{Si} is created. This leads us to propose a simple process that can indeed lead to copper precipitates starting with a single $Cu_{s1}Cu_{i4}$. We show that it can easily become $Cu_{s2}Cu_{i3}$, which attracts Cu_i leading to further copper precipitation. The structures, binding energies, and gap levels are predicted up to $Cu_{s2}Cu_{i6}$. The path toward larger aggregates is outlined. We try to correlate the calculated electrical properties of these complexes with any new defect levels found by DLTS in specially prepared Cu doped samples.

Section II deals with the methodology, both theoretical and experimental. Section III contains the results starting with calculated and measured properties of $Cu_{s1}Cu_{in}$. Then, we discuss V_{Si} formation energies and its dependence on where it is created. The theory part concludes with a discussion of the evolution of the copper precipitate. Then, the experimental results in p-type Si and n-type Si are given. Section IV contains a discussion of the key results.

II. METHODOLOGY

A. Theory

Our spin-density-functional calculations are based on the SIESTA method[34,35] in Si_{216} periodic supercells. This approach has been used successfully for other 3d TM impurities: Ti,[4,36] V,[37] Fe,[37–40] Ni,[41] Cu,[6,42] and Co.[43] The lattice constant of the impurity-free cell is optimized in each charge state, and the defect geometries are obtained with a conjugate gradient algorithm. A $3 \times 3 \times 3$ Monkhorst-Pack[44] mesh is used to sample the Brillouin zone. The electronic core regions are removed from the calculations using the Troullier–Martins norm-conserving pseudopotentials[45] developed for SIESTA.[46] All the pseudopotentials have relativistic and core corrections.

The Cu pseudopotential includes semicore 3s and 3p states. The valence regions are treated with spin-density-functional theory within the revised generalized gradient approximation for the exchange-correlation potential.[47] This potential leads to the prediction of accurate activation energies for diffusion of impurities in Si.[48] The charge density is projected on a real-space grid with an equivalent cutoff of 350 Ryd to calculate the exchange-correlation and Hartree potentials. The basis sets for the valence states are linear combinations of numerical atomic orbitals:[49,50] double-zeta for the first two rows of the Periodic Table with a set of polarization functions (five 3d's) for Si. The basis set of Cu includes two sets of s and d orbitals and one set of p's.

The structures of the multi-copper complexes were optimized in each charge and spin state using a conjugate-gradient algorithm until the maximum force component is smaller than 0.003 eV/Å. This was done starting with a range of *a priori* plausible initial configurations. The configurations discussed below are the ones with the lowest-energy spin state for each charge state.

The gap levels are evaluated using the formation energies[51] vs electron chemical potential as well as the marker method.[52,53] For Cu-related defects, the gap levels calculated with both methods are within 0.01 eV of each other (only two of 18 donor or acceptor levels differ by 0.01 eV, all the other ones match almost perfectly). In the marker method, the donor (acceptor) levels are obtained relative to the top (bottom) of the valence (conduction) band. The experimental gap is only used when plotting the levels. The perfect crystal is used as the universal marker: the references for donor and acceptor levels are the top of the valence band and the bottom of the conduction band, respectively. This implementation of the marker method works well for a wide range of defects provided that the defect geometries and the lattice constant of the supercell are optimized in each charge state with a $3 \times 3 \times 3$ k-point sampling. This produces converged energies for the supercell size used here.

B. Experiment

The samples used in the present work were cut from p-type Si and n-type Si floating-zone Si single crystals that were

co-doped with copper during growth.[7,9] The Cu_s concentration was $\sim 5-10\times10^{13}$ cm^{-3}, while the total amount of copper in the samples was about ten times higher.

These as-received crystals were annealed at 150–650 °C and then etched in a CP4 acid solution as described in Ref. 10. Then, Cu_i was introduced at room temperature by chemo-mechanical polishing (CMP) in a standard silica slurry contaminated with Cu.[12,54] The deep-level spectra were obtained using the standard (DLTS) or high resolution (LDLTS) capacitance techniques.[55] Capacitance measurements were performed at a frequency of 1 MHz. LDLTS with two filling pulses was used to determine the activation enthalpies and capture cross sections of the deep levels and their depth profiles. Schottky diodes were prepared by Al (p-type) or Au (n-type) vacuum deposition through a shadow mask. The ohmic contacts were prepared with an InGa paste. We label DLTS peaks according to electron (E) or hole (H) traps and the temperature of the peak maximum at the emission rate of 50 s^{-1}.

III. RESULTS

A. From Cu_i to $Cu_{s1}Cu_{i4}$: Theory

Our calculated results are consistently close to those obtained by Carvalho *et al.*[6] Therefore, no "in-depth" discussion is needed, and we simply summarize the key results. However, we do consider the possibility that double-donor or double-acceptor levels are present in the gap. The rapidly diffusing Cu_i is stable at the tetrahedral interstitial (T) site. Its donor level is very high in the gap at $E_v + 0.85$ eV. We also find an acceptor level at $E_c - 0.14$ eV. Thus, in p-type and intrinsic Si, interstitial copper is Cu_i^+ (spin 0) and becomes Cu_i^0 (spin 1/2) and then Cu_i^- (spin 0) in heavily doped n-Si.

The reaction with a pre-existing V_{Si} leads to the formation of Cu_s with a net gain in energy corresponding to the formation of four Cu_s–Si bonds with bond strength of 0.78 eV each: $Cu_i^0 + V^0 \rightarrow Cu_s^0 + 3.12$ eV. The lattice distortion around Cu_s is very small (less than 0.01 Å), but the Cu–Si bonds are much weaker than the Si–Si bonds in the perfect crystal, which will be important further below. As mentioned above, the calculated gap levels of Cu_s lead to the following charge (spin) states: Cu_s^+ (spin 1) in heavily doped p-type Si, Cu_s^0 (spin 3/2) in p-type Si, but Cu_s^- (spin 1) or Cu_s^{2-} (spin 1/2) for other positions of the Fermi level.

The interaction between Cu_i^+ and Cu_s leads to the formation of $Cu_{s1}Cu_{i1}$ (with Cu_i very near to one of the four T sites next to Cu_s), then $Cu_{s1}Cu_{i2}$ (with the Cu_is very near to two of the four T sites next to Cu_s), and finally $Cu_{s1}Cu_{i3}$ (with the Cu_i's very near to three of the four T sites next to Cu_s). The calculated gap levels of these complexes are shown in Fig. 1.

The calculated energy gains at each step for the specified charge states are as follows: $Cu_i^+ + Cu_s^- \rightarrow Cu_{s1}Cu_{i1}^0 + 0.79$ eV. If the Fermi level is mid- or above midgap, $Cu_{s1}Cu_{i1}^0$ will trap an electron and become $Cu_{s1}Cu_{i1}^-$. Then, $Cu_i^+ + Cu_{s1}Cu_{i1}^- \rightarrow Cu_{s1}Cu_{i2}^0 + 0.77$ eV. For the same Fermi level positions, this complex will trap an electron and become $Cu_{s1}Cu_{i2}^-$; $Cu_i^+ + Cu_{s1}Cu_{i2}^- \rightarrow Cu_{s1}Cu_{i3}^0 + 0.69$ eV, which remains in the 0 charge state. The lowest-energy spin states of $Cu_{s1}Cu_{i3}$ are 0, 1/2, 0, and 1/2 in the 2+, +, 0, and − charge states, respectively. Note that the binding (and dissociation) energies are expected to be charge-state dependent.

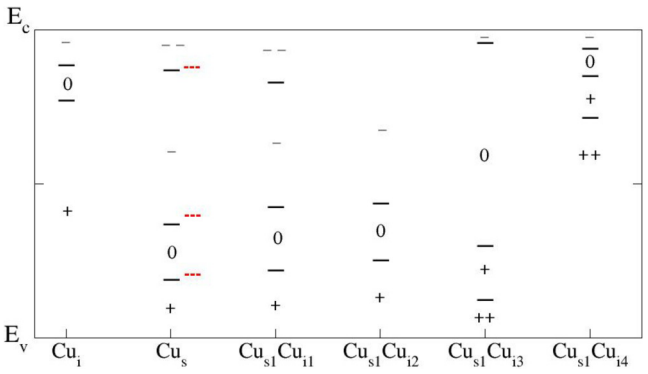

FIG. 1. The solid (black) lines show the calculated gap levels of Cu_i, Cu_s, $Cu_{s1}Cu_{i1}$, $Cu_{s1}Cu_{i2}$, $Cu_{s1}Cu_{i3}$, and $Cu_{s1}Cu_{i4}$. The experimental data for Cu_s are dotted (red) lines.[7–10] Note that $Cu_{s1}Cu_{i1}$ has a double-acceptor level while $Cu_{s1}Cu_{i3}$ and $Cu_{s1}Cu_{i4}$ have a double-donor level in the gap. The donor (acceptor) levels are calculated relative to the top (bottom) of the valence (conduction) band. The low-temperature gap at 4.2 K is 1.17 eV.

There are four T sites adjacent to Cu_s. Even though there is no Coulomb attraction between $Cu_{s1}Cu_{i3}^0$ and Cu_i^+, a fourth Cu_i can still trap, albeit with a smaller binding energy: $Cu_i^+ + Cu_{s1}Cu_{i3}^0 \rightarrow Cu_{s1}Cu_{i4}^+ + 0.61$ eV. As shown in Fig. 1, the final complex is in the + or 2+ charge state, repels Cu_i^+, and the complex should no longer grow.

B. Cu precipitation starting with $Cu_{s1}Cu_{i4}$: Theory

As shown in Fig. 1, the donor and acceptor levels of Cu_i are very high in the gap, and they drop considerably when V_{Si} is added and Cu_s forms. Adding one V_{Si} to $Cu_{s1}Cu_{i4}$ would result in the formation of $Cu_{s2}Cu_{i3}$. The second Cu_s is likely to drive the gap levels down within the gap, thus possibly changing the charge state of the defect. While $Cu_{s1}Cu_{i4}$ is almost always in the + or 2+ charge states, thus repelling Cu_i^+, the $Cu_{s2}Cu_{i3}$ complex can be in 0 or even −1 charge states (see below) and therefore trap more Cu_is. However, the formation energy of V_{Si} is of the order of 3.5–4.2 eV,[56–59] making it highly unlikely that it will spontaneously form at room temperature.

However, V_{Si} formation energy strongly depends on where it is created. In perfect Si and for a neutral V_{Si}, $E_{form}(V_{Si}) = 3.72$ eV at the present level of theory. But if the Si atom removed is an NN to Cu_i^+, the number drops to 3.19 eV: because it is positively charged, Cu_i^+ attracts some electron density from the nearest Si–Si bonds, thus weakening these bonds and making them easier to remove an Si atom. Then, as $Cu_i + V_{Si} \rightarrow Cu_s$, the energy cost drops to 0.82 eV as shown in Fig. 2. If V_{Si} is created next to Cu_s, then the energy cost drops to 2.16 eV. Here, the reason is that one does not need to break four strong Si–Si bonds but only three of them plus one, much weaker, Cu–Si bond. If V_{Si} is created next to $Cu_{s1}Cu_{i3}$, the energy cost is even less, ∼1.7 eV, because of the combined effect of having one Cu_s (i.e., one weak Cu–Si bond) and three Cu_is (which weaken the neighboring Si–Si bonds). But then, if one of the Cu_is becomes Cu_s, the net energy cost to form $Cu_{s2}Cu_{i2}$ starting with

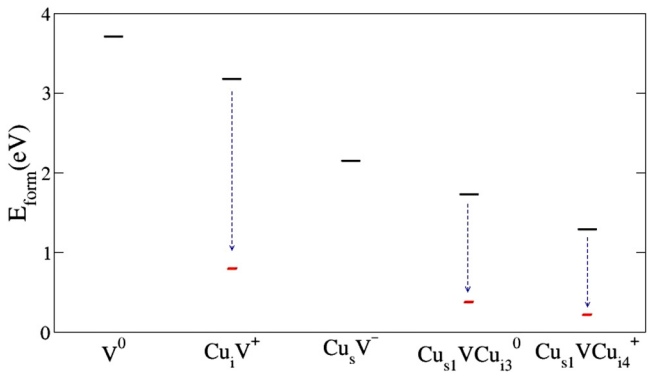

FIG. 2. Calculated formation energies of V_{Si} if an Si atom is removed (left to right) from the perfect Si (V^0), from a site NN to Cu_i^+ (Cu_iV^+), to Cu_s^- (Cu_sV^-), to $Cu_{s1}Cu_{i3}^0$ ($Cu_{s1}VCu_3^0$), or to $Cu_{s1}Cu_{i4}^+$ ($Cu_{s1}VCu_{i4}^+$). The vertical dashed (blue) lines show the subsequent energy drop when Cu_i becomes Cu_s, forming Cu_s, $Cu_{s2}Cu_{i2}$, and $Cu_{s3}Cu_{i3}$.

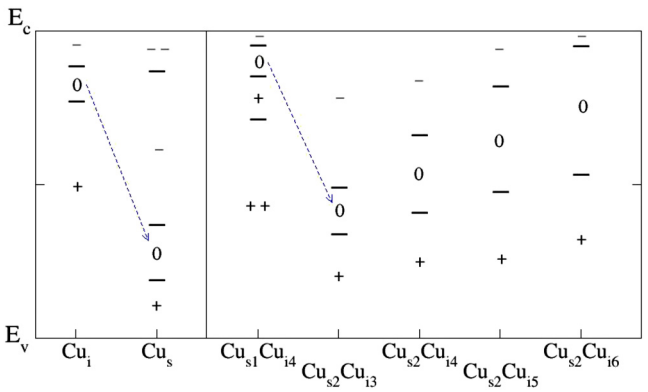

FIG. 3. The solid (black) lines show the calculated gap levels of Cu_i, Cu_s, and then $Cu_{s1}Cu_{i4}$, $Cu_{s2}Cu_{i3}$, $Cu_{s2}Cu_{i4}$, $Cu_{s2}Cu_{i5}$, and $Cu_{s2}Cu_{i6}$. The drop in the energy levels that occurs when Cu_i becomes Cu_s is emphasized with dashed (blue) arrows. The donor (acceptor) levels are calculated relative to the top (bottom) of the valence (conduction) band. The low-temperature gap at 4.2 K is 1.17 eV.

$Cu_{s1}Cu_{i3}$ drops to 0.39 eV. Finally, next to $Cu_{s1}Cu_{i4}$, the total energy balance is even more favorable, 0.23 eV. Thus, the probability of forming V_{Si} is considerably greater right next to $Cu_{s1}Cu_{i3}$ or $Cu_{s1}Cu_{i4}$ than far away from it, especially if one factor in the energy gained when one of the Cu_i jumps into V_{Si} and forms Cu_s.

There is indirect experimental support for one of these reactions from electron-irradiation experiments. In samples that contain no copper, e^- irradiation results in the formation of A-centers (O–V_{Si} pairs), but when the same sample contains Cu_i, e^- irradiation results in the formation of Cu_s and no A-center is seen.[60] One could argue that Cu_i diffuses much faster toward V_{Si} than V_{Si} can diffuse toward interstitial O (O_i). On the other hand, V_{Si} could simply be created next to Cu_i at a lower cost than far from it. Note that creating V_{Si} by removing an Si atom NN to Cu_i^+ and forming the $Cu_i^+V_{Si}^0$ pair produces an energy gain of 0.53 eV. On the other hand, it *costs* more energy to remove a Si atom NN to O_i (and forming $O_i^0V_{Si}^0$) than in the perfect crystal because one needs to break three Si–Si bonds and one, much stronger, Si–O bond. More calculations of these processes are needed. A very similar argument has been made by Sueoka *et al.*[61] about V_{Si} and self-interstitial formation in CZ-Si.

These V_{Si} formation energy calculations show that—should V_{Si} be created—it is most likely to occur right next to $Cu_{s1}Cu_{i4}$ and result in the formation of $Cu_{s2}Cu_{i3}$. As expected, the creation of a second Cu_s causes the gap levels to drop in the gap, changing the charge state of $Cu_{s1}Cu_{i4}^+$ into $Cu_{s2}Cu_{i3}^-$ (for Fermi-level positions near midgap). Then, as we add more Cu_is, the donor and acceptor levels again steadily rise in the gap until the defect becomes positively charged again, and a new V_{Si} needs to be created.

Figure 3 shows the calculated gap levels of $Cu_{s2}Cu_{i3}$, $Cu_{s2}Cu_{i4}$, $Cu_{s2}Cu_{i5}$, and $Cu_{s2}Cu_{i6}$ (Fig. 4). As anticipated (above), the donor and acceptor levels drop substantially when $Cu_{s1}Cu_{i4}$ becomes $Cu_{s2}Cu_{i3}$. This causes the charge state of the defect to change from + (or 2+) to 0 or −, making it attractive to Cu_i^+. As the defect grows by the addition of new interstitial copper atoms, the levels steadily climb in the gap until $Cu_{s2}Cu_{i6}$, when a new V_{Si} should be created for the reaction to continue. The calculated binding energies are $Cu_i^+ + Cu_{s2}Cu_{i3}^- \rightarrow Cu_{s2}Cu_{i4}^0 + 0.75$ eV; $Cu_i^+ + Cu_{s2}Cu_{i4}^0 \rightarrow Cu_{s2}Cu_{i5}^+ + 0.77$ eV; and $Cu_i^+ + Cu_{s2}Cu_{i5}^0 \rightarrow Cu_{s2}Cu_{i6}^+ + 0.73$ eV. Note that the $Cu_{s2}Cu_{i6}$ complex is more stable by 0.40 eV if the two Cu_i's are second-NNs (Cu_s–Si–Cu_s) rather than adjacent to each other.

Note that our argument focuses on the formation of V_{Si}. Of course, when creating V_{Si}, one also creates a self-interstitial (I_{Si}). Since we did not find any energetically favorable {Cu,I_{Si}} complex, we assume that I_{Si} is repelled by the Cu environment and diffuses away toward some energetically favorable sites such as substitutional C or another self-interstitial.

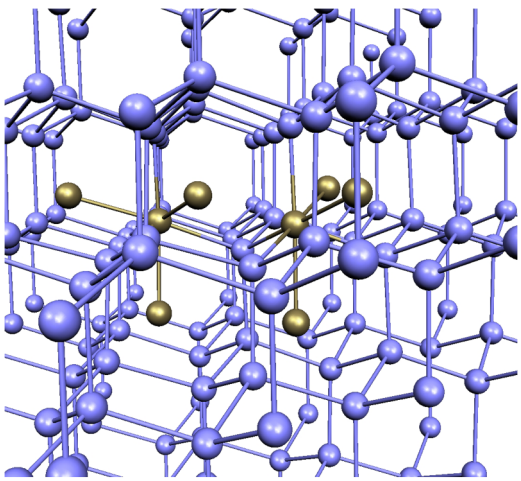

FIG. 4. The $Cu_{s2}Cu_{i6}$ complex. The Cu atoms are golden and the Si atoms are light blue.

C. From Cu_s to Cu_{PL}: Experiment

The measurements were performed on Si samples doped with Cu during the float-zone growth.[7,9] The 1-mm thick wafers were cut from the boules and kept at room temperature for many years. The typical DLTS curve measured from the as-received p-type sample is shown in Fig. 5(a). The spectrum is dominated by the H49 peak at $E_v + 0.10$ eV. This center was correlated with the zero-phonon PL line at 1014 meV[22] known as Cu_{PL} that contains (at least) four Cu atoms.[30,31] Additional peaks are seen in the 100–140 K and 200–250 K temperature ranges. The LDLTS technique resolves the signals into three levels in the 0.18–0.26 eV energy range and two levels around 0.45 eV.

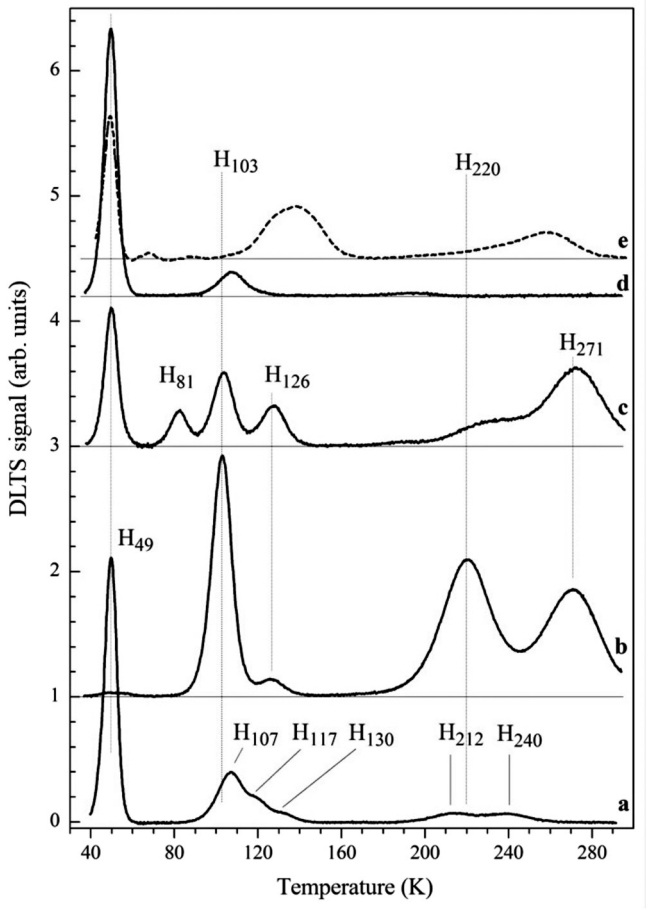

FIG. 5. DLTS curves (rate window: 49 s^{-1}) in p-type Si:Cu samples after following treatments: (a) as received; (b) after annealing at 350 °C for 30 min; (c) 30 s CMP in the Cu-contaminated slurry; (d) 5 min CMP in the Cu-contaminated slurry; and (e) aging at 150 °C for 13 h after quenching from 650 °C. Samples (a), (b), and (e) were subjected to a deep acid chemical etching before the diode deposition. All curves were taken from the hydrogen-free region, 2–4 μm from the treated surface.

TABLE I. Activation energies E_a and apparent capture cross section σ obtained by fitting the Arrhenius curves with the standard T^2 correction.

DLTS level	E_a (eV)	σ (10^{-15} cm^2)	Identification
E107	$E_c - 0.16$	0.024	Cu_s (second acceptor)
H271	$E_v + 0.55$	3.4	$Cu_{s1}Cu_{i1}$ (acceptor)
H220	$E_v + 0.43$	2.0	Cu_s (acceptor)
H126	$E_v + 0.27$	66	$Cu_{s1}Cu_{i2}$ (donor)
H103	$E_v + 0.23$	140	Cu_s (donor)
H102	$E_v + 0.21$	21	$Cu_{s1}Cu_{i1}$ (donor)
H49	$E_v + 0.10$	110	Cu_{PL} (donor)

Annealing at 350 °C results in disappearance of the H49 center. Instead, the H103 and H220 peaks appear [Fig. 5(b)]. These are related to the donor and acceptor levels of Cu_s.[7,8] The difference in the amplitudes of the H103 and H220 peaks is due to the presence of another defect whose acceptor level is responsible for the H271 peak while the signal from the donor H102 level contributes to the H103 peak.[9,12] The parameters obtained from the Arrhenius plots of the hole emission rates are shown in Table I. The H102/H271 center decreases away from the surface and is believed to form because of the chemical etching before the diode deposition. Another feature seen in the curve (b) is the H126 peak. It is always rather small and the corresponding centers are close to the etched surface.

All the curves in Fig. 5 were taken from the region deeper than ~2 μm from the treated surface. This excludes any effect of hydrogen as its diffusion length (determined by the formation of H–B pairs) is about 0.15 – 0.2 μm in our samples. Therefore, the defects formed as a result of chemical etching are related to another fast-diffusing species that does not form a stable complex with boron. It is reasonable to assume that it is Cu_i that is highly mobile (the lifetime of the Cu_i–B pair is only ~1 ms at room temperature[3]). Therefore, the H102/H271 signals are assigned to $Cu_{s1}Cu_{i1}$ (Ref. 12) while the H126 feature is tentatively assigned to $Cu_{s1}Cu_{i2}$. No other center is present in significant concentration.

Whatever the mechanism of Cu_i formation on the surface during etching, a quasi-stationary distribution of in-diffusing particles and Cu-related complexes is quickly established due to the motion of the surface during etching.[62] Indeed, the spectrum in Fig. 5(b) remains stable, independent of the etching time above 1 min. Therefore, to proceed with formation of higher-order complexes, another source of Cu_i is required. It is known that mobile copper species can be introduced during the CMP in a Cu-contaminated slurry (the surface movement is negligible in this case). The DLTS curve measured after short CMP is shown in Fig. 5(c). The Cu_{PL} (H49) center is already in its highest concentration, as Cu_s centers are nearly absent (see the signal amplitude at 220 K). The $Cu_{s1}Cu_{i1}$ (H102/H271) and $Cu_{s1}Cu_{i2}$ (H126) signals are also strong. The H81 peak has been attributed[12] to a Cu_sCu_{i2} complex as its formation consumed one Cu_s. However, it was later shown[63] that the complex includes Ni introduced from the contaminated slurry. Polishing for longer times results in the dominance of Cu_{PL} [Fig. 5(d)]. Further, a signal at 107 K similar to that observed in the as-received samples is formed.

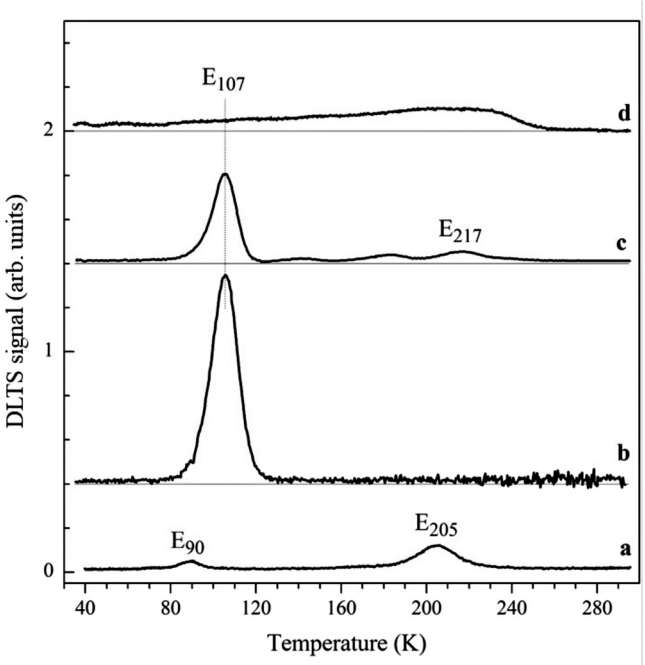

FIG. 6. DLTS curves (rate window: 49 s^{-1}) measured in n-type Si:Cu crystals after following treatments: (a) as received; (b) 30 min annealing at 350 °C + mechanical polishing; (c) sample (b) +2 min CMP in the Cu-contaminated slurry; and (d) annealing at 650 °C + fast cooling. All curves were taken 2–4 μm from the surface.

We have tried to model the processes that occur during many years of storage at room temperature. A uniform concentration of Cu_{PL} centers was created by quenching from high temperature (650 °C). Then the sample was heat treated at 150 °C for 13 h, a process that should not affect the Cu_{PL} concentration.[8] However, the measured Cu_{PL} concentration was about half that found after the 650 °C annealing. Instead, a set of new levels appeared with energies in the 0.2–0.3 and 0.5–0.6 eV ranges above the valence band [Fig. 5(e)]. These levels differ from those formed at room temperature (both due to long storage and CMP). The associated defects were uniformly distributed in depth and showed a normal (pointlike) behavior with respect to varying DLTS rate window and filling pulse duration. For these reasons, these centers cannot be related to extended defects (precipitates).

The DLTS results obtained in n-type samples doped with copper during growth are shown in Fig. 6. Only few rather weak DLTS signals were detected in the as-received samples [Fig. 6(a)]. The concentration of these homogeneously distributed defects cannot account for the expected Cu_s concentration. This observation correlates with the results in p-type, where all Cu_s atoms were included into the Cu_{PL} centers.

Figure 6(b) shows a spectrum after a 350 °C anneal that is known to destroy Cu_{PL}. In n-type Si, the separation between pure Cu defects and the Cu–H complexes that are formed during chemical etching is more difficult to achieve than in p-type Si due to the deeper H in-diffusion. To avoid any H-related effect, the sample was mechanically polished after annealing with a diamond paste before contact preparation. And then, only the E107 peak is seen, the Cu_s second acceptor level.[7,8]

Introducing Cu_i by CMP reduces the Cu_s concentration. A 2 min polishing results in decrease of E107 by more than a factor of 2 and several new peaks appear [Fig. 6(c)]. Increasing the CMP time to 10–20 min results in the disappearance of all deep levels from the upper half of the gap (not shown).

The curve Fig. 6(d) was measured after annealing of the copper-doped n-type sample at 650 °C and fast cooling. Only a weak and broad DLTS signal was observed, which could be related with copper precipitates. The low-temperature PL measured from this sample showed a strong Cu_{PL} 1014 meV line, showing that Cu_{PL} has no deep-levels in the upper half of the gap, in agreement with the statement in Ref. 64. Table I summarizes the properties of the Cu-related DLTS peaks in this study.

IV. SUMMARY AND DISCUSSION

Copper precipitation in intrinsic Si is not understood. The present theoretical/experimental study focuses on two issues related to this issue: First, the Cu_{PL} defect and the nature of the intermediate complexes, and second, a mechanism for the growth of Cu precipitates in intrinsic Si beyond Cu_{PL}. A summary of the gap levels predicted by theory and observed by DLST is in Table II.

It is well established from PL studies that Cu_{PL} contains (at least) four Cu atoms, and annealing studies have shown that the core of Cu_{PL} is isolated Cu_s. The first intermediate complex identified here forms following the wet chemical etching (WCE) of Cu-doped samples and is characterized by the H102 ($E_v + 0.21$ eV) donor and H271 ($E_v + 0.55$ eV) acceptor levels. They closely match the calculated levels of $Cu_{s1}Cu_{i1}$ at $E_v + 0.23$ eV and $E_c - 0.65$ eV (Fig. 1 and Table II). These two lines were originally ascribed to the {Cu_s,H} pair.[9] However, H cannot penetrate deeper than ~1 μm, while the H102/H271 DLTS peaks are observed much deeper in the sample (~3–5 μm). Further, the sum of H103/H220 (Cu_s) and H102/H271 ($Cu_{s1}Cu_{i1}$) exhibits a flat profile that matches the initial Cu_s concentration. Moreover, the characteristic depth of the H102/H271 center after WCE is about 2 μm, which fits the Cu_i diffusion length with respect to capture by the given Cu_s concentration with a capture radius of about 0.3 nm. The latter is characteristic of interactions when at least one particle is neutral (here, Cu_s). The H102/H271 center is stable for hours (days) at room temperature and for minutes at 340 K. This corresponds to a 0.8–1.0 eV dissociation energy (the calculated binding energy is 0.77 eV).

The H81 DLTS peak was first proposed to be a three-Cu complex[12] but was later shown to be Ni-related.[63] A candidate for the $Cu_{s1}Cu_{i3}$ center is H126 ($E_v + 0.27$ eV). The fact that this level is observed closer to the etched surface and occurs in smaller concentrations than the H102/H271 center[9] supports this assignment. Further, the total acceptor level concentration calculated as H220 (Cu_s) + H271 ($Cu_{s1}Cu_{i1}$) equals H126 ($Cu_{s1}Cu_{i2}$) + H103/H102 ($Cu_s/Cu_{s1}Cu_{i1}$): adding H126 to H103/H102 extends the flat profile of the total Cu_s concentration closer to the surface. Finally, the measured donor level is very close to the calculated one (Table II).

TABLE II. Calculated (measured or measured range) gap levels (in electron volts) associated with all the defects in this study. The donor levels are evaluated relative to the valence band and the acceptor levels relative to the conduction band.

Defect	(+/+ +)	(0/+)	(−/0)	(− −/−)
Cu_i		$E_v + 0.85$	Ec − 0.14	
Cu_s		$E_v + 0.20$ (0.20–0.23)	Ec − 0.72 (0.68–0.74)	Ec − 0.16 (0.16)
$Cu_{s1}Cu_{i1}$		$E_v + 0.23$ (0.21)	Ec − 0.65 ($E_v + 0.55$)	Ec − 0.20
$Cu_{s1}Cu_{i2}$		$E_v + 0.27$ (0.27)	Ec − 0.64	
$Cu_{s1}Cu_{i3}$	$E_v + 0.13$	$E_v + 0.30$	Ec − 0.03	
$Cu_{s1}Cu_{i4}$	$E_v + 0.79$	$E_v + 0.94$	Ec − 0.06	
$Cu_{s2}Cu_{i3}$		$E_v + 0.40$	Ec − 0.65	
$Cu_{s2}Cu_{i4}$		$E_v + 0.45$	Ec − 0.39	
$Cu_{s2}Cu_{i5}$		$E_v + 0.52$	Ec − 0.21	
$Cu_{s2}Cu_{i6}$		$E_v + 0.59$	Ec − 0.07	

This suggests that the three-Cu center also has an acceptor level, but its DLTS signature would be hidden under the strong H220 or H271 peak (the calculated position suggests H271). The presence of the acceptor level is in good agreement with the calculated $E_c - 0.64$ eV level of $Cu_{s1}Cu_{i2}$. Finally, the H126 level is slightly less stable than the H102/H271 center, and theory predicts a binding energy of 0.69 eV, slightly less than that of $Cu_{s1}Cu_{i1}$.

After such a good correlation between experiment and theory, it is surprising that the calculated single-donor level of $Cu_{s1}Cu_{i3}$ ($E_v + 0.30$ eV, and even higher in Ref. 32) is quite different from the Cu_{PL} donor level at $E_v + 0.10$ eV. Moreover, DLTS experiments show no sign of the calculated double-donor level at $E_v + 0.13$ eV (the calculated acceptor at $E_c - 0.03$ eV is too shallow to be reliable). In the samples with the strongest Cu_{PL} photoluminescence, only the $E_v + 0.10$ eV level is detected both in p- and in n-type samples. Finally, the Cu_{PL} DLTS level exhibits a much higher thermal stability than the two-Cu and three-Cu centers discussed above ($Cu_{s1}Cu_{i1}$ and $Cu_{s1}Cu_{i2}$), while theory predicts a binding energy of 0.69 eV for $Cu_{s1}Cu_{i3}$, close to that of the two smaller clusters.

Theory shows a steady trend in the evolution of the gap levels from Cu_s to $Cu_{s1}Cu_{i3}$ (Fig. 1): the capture of each new Cu_i results is the steady rise of the levels in the gap, and the same trend is seen starting with $Cu_{s2}Cu_{i3}$ (Fig. 3). It would be difficult to explain why the single-donor level of $Cu_{s1}Cu_{i3}$ would suddenly drop down to 0.10 eV.

One could speculate that some dramatic reorientation of $Cu_{s1}Cu_{i3}$ occurs into a different trigonal configuration, but no such reorientation has been found by theorists so far. It could also be that the PL with zero-phonon line at 1014 meV and the DLTS peak at $E_v + 0.10$ eV are actually associated with two different Cu clusters. This would imply that Cu has more than one way to precipitate in defect-free Si. For example, substitutional carbon (C_s) is always present and it is *a priori* possible to imagine a trigonal center such as C_s–Cu_s–(Cu_{i3}). The added C atom would not necessarily participate in the local vibrational mode associated with the Cu_{PL} isotope splitting. This possibility was not considered here.

However, we examined theoretically the possibility that $Cu_{s1}Cu_{i4}$ can continue to grow. Because this complex is in the + or 2+ charge state for most positions of the Fermi level, it cannot trap additional Cu_i^+s. V_{Si} must be created to generate a second Cu_s, thus altering the gap levels and changing the charge state of the defect. The formation energy of the V_{Si} was shown to depend strongly on *where* it is created. In particular, V_{Si} can be created very close to $Cu_{s1}Cu_{i4}$ at a low cost in energy. This results in one Cu_i becoming Cu_s and $Cu_{s1}Cu_{i4}$ becoming $Cu_{s2}Cu_{i3}$. Each time one interstitial copper becomes substitutional, the defect levels drop within the gap and the defect changes charge for most positions of the Fermi level, thus allowing further Cu precipitation. This process will require new experimental studies but several new gap levels have been predicted.

ACKNOWLEDGMENTS

T.M.V. and S.K.E. received a large amount of computer time from Texas Tech's High-Performance Computer Center and UT's Texas Advanced Computer Center in Austin, TX. This project was supported in part by the Deutsche Forschungsgemeinschaft under Contract No. WE 1319/19. The work in IMT RAS was performed within the state Task No. 075-00475-19-00.

REFERENCES

[1]A. A. Istratov and E. R. Weber, Appl. Phys. A **66**, 123 (1998).
[2]D. E. Woon, D. S. Marynick, and S. K. Estreicher, Phys. Rev. B **45**, 13383 (1992).
[3]A. A. Istratov, C. Flink, H. Hieslmair, E. R. Weber, and T. Heiser, Phys. Rev. Lett. **81**, 1243 (1998).
[4]D. J. Backlund and S. K. Estreicher, Phys. Rev. B **81**, 235213 (2010).
[5]A. A. Istratov, H. Hieslmair, C. Flink, T. Heiser, and E. R. Weber, Appl. Phys. Lett. **71**, 2349 (1997).
[6]A. Carvalho, D. J. Backlund, and S. K. Estreicher, Phys. Rev. B **84**, 155322 (2011).
[7]H. Lemke, Phys. Status Solidi A **95**, 665 (1986).
[8]S. D. Brotherton, J. R. Ayres, A. Gill, H. W. van Kesteren, and F. J. M. Greidanus, J. Appl. Phys. **62**, 1826 (1987).
[9]S. Knack, J. Weber, H. Lemke, and H. Riemann, Phys. Rev. B **65**, 165203 (2002).
[10]N. Yarykin and J. Weber, Phys. Rev. B **88**, 085205 (2013).
[11]K. Shirai, H. Yamaguchi, A. Yanase, and H. Katayama-Yoshida, J. Phys. Condens. Matter **21**, 064249 (2009).
[12]N. Yarykin and J. Weber, Semiconductors **47**, 275 (2013).
[13]W. C. Dash, J. Appl. Phys. **27**, 1193 (1956).

[14]S. M. Myers and D. M. Follstaedt, J. Appl. Phys. **79**, 1337 (1996).
[15]S. McHugo, A. Mohammed, A. C. Thompson, B. Lai, and Z. Cai, J. Appl. Phys. **91**, 6396 (2002).
[16]C. Flink, H. Feick, S. McHugo, W. Seifert, H. Hieslmair, T. Heiser, A. A. Istratov, and E. R. Weber, Phys. Rev. Lett. **85**, 4900 (2000).
[17]A. A. Istratov, H. Hedeman, M. Seibt, O. F. Vyvenko, W. Schröter, T. Heiser, C. Flink, H. Hieslmair, and E. R. Weber, J. Electrochem. Soc. **145**, 3889 (1998).
[18]T. Buonassisi, M. A. Marcus, A. A. Istratov, M. Heuer, T. F. Ciszek, B. Lai, Z. Cai, and E. R. Weber, J. Appl. Phys. **97**, 063503 (2005).
[19]N. S. Minaev, A. V. Mudryi, and V. D. Tkachev, Fiz. Tekh. Poluprovodn. **13**, 395 (1979) [Sov. Phys. Semicond. **13**, 233 (1979)].
[20]J. Weber, H. Bauch, and R. Sauer, Phys. Rev. B **25**, 7688 (1982).
[21]M. H. Nazaré, A. J. Duarte, A. G. Steele, G. Davies, and E. C. Lightowlers, Mater. Sci. Forum **83–87**, 191 (1992).
[22]H. B. Erzgräber and K. Schmalz, J. Appl. Phys. **78**, 4066 (1995).
[23]M. Nakamura, Appl. Phys. Lett. **73**, 3896 (1998).
[24]A. A. Istratov, H. Hieslmair, T. Heiser, C. Flink, and E. R. Weber, Appl. Phys. Lett. **72**, 474 (1998).
[25]M. Nakamura and S. Murakami, J. Appl. Phys. **111**, 073512 (2012).
[26]N. Yarykin and J. Weber, Appl. Phys. Lett. **105**, 012109 (2014).
[27]S. Knack, J. Weber, H. Lemke, and H. Riemann, Physica B **308-310**, 404 (2001).
[28]S. Knack, Mater. Sci. Semicond. Process. **7**, 125 (2004).
[29]S. K. Estreicher, D. West, J. Goss, S. Knack, and J. Weber, Phys. Rev. Lett. **90**, 035504 (2003).
[30]M. Steger, A. Yang, N. Stavrias, M. L. W. Thewalt, H. Riemann, N. V. Abrosimov, M. F. Churbanov, A. V. Gusev, A. D. Bulanov, I. D. Kovalev, A. K. Kaliteevskii, O. N. Godisov, P. Becker, and H.-J. Pohl, Phys. Rev. Lett. **100**, 177402 (2008).
[31]M. Steger, A. Yang, T. Sekiguchi, K. Saeedi, M. L. W. Thewalt, M. O. Henry, K. Johnston, H. Riemann, N. V. Abrosimov, M. F. Churbanov, A. V. Gusev, A. K. Kaliteevskii, O. N. Godisov, P. Becker, and H.-J. Pohl, J. Appl. Phys. **110**, 081301 (2011).
[32]A. Sharan, Z. Gui, and A. Janotti, Phys. Rev. Appl. **8**, 024023 (2017).
[33]Y. Ohno, K. Inoue, K. Kutsukake, M. Deura, T. Ohsawa, I. Yonenaga, H. Yoshida, S. Takeda, R. Taniguchi, H. Otubo, S. R. Nishitani, N. Ebisawa, Y. Shimizu, H. Takamizawa, K. Inoue, and Y. Nagai, Phys. Rev. B **91**, 235315 (2015).
[34]D. Sánchez-Portal, P. Ordejón, E. Artacho, and J. M. Soler, Int. J. Quant. Chem. **65**, 453 (1997).
[35]E. Artacho, D. Sánchez-Portal, P. Ordejón, A. García, and J. M. Soler, Phys. Status Solidi B **215**, 809 (1999).
[36]D. J. Backlund and S. K. Estreicher, Phys. Rev. B **82**, 155208 (2010).
[37]D. J. Backlund, T. M. Gibbons, and S. K. Estreicher, Phys. Rev. B **94**, 195210 (2016).
[38]M. Sanati, N. Gonzalez Szwacki, and S. K. Estreicher, Phys. Rev. B **76**, 125204 (2007).
[39]S. K. Estreicher, M. Sanati, and N. Gonzalez Szwacki, Phys. Rev. B **77**, 125214 (2008).
[40]N. Gonzalez Szwacki, M. Sanati, and S. K. Estreicher, Phys. Rev. B **78**, 113202 (2008).
[41]J. Lindroos, D. P. Fenning, D. Backlund, E. Verlage, A. Gorgulla, S. K. Estreicher, H. Savin, and T. Buonassisi, J. Appl. Phys. **113**, 204906 (2013).
[42]D. West, S. K. Estreicher, S. Knack, and J. Weber, Phys. Rev. B **68**, 035210 (2003).
[43]T. M. Gibbons, D. J. Backlund, and S. K. Estreicher, J. Appl. Phys. **121**, 045704 (2017).
[44]H. J. Monkhorst and J. D. Pack, Phys. Rev. B **13**, 5188 (1976).
[45]N. Troullier and J. L. Martins, Phys. Rev. B **43**, 1993 (1991).
[46]P. Rivero, V. M. García-Suárez, D. Pereñiguez, K. Utt, Y. Yang, L. Bellaiche, K. Park, J. Ferrer, and S. Barraza-Lopez, Comput. Mater. Sci. **98**, 372 (2015).
[47]B. Hammer, L. Hansen, and J. K. Nørskov, Phys. Rev. B **59**, 7413 (1999).
[48]S. K. Estreicher, D. J. Backlund, C. Carbogno, and M. Scheffler, Angew. Chem. **50**, 10221 (2011).
[49]O. F. Sankey and D. J. Niklewski, Phys. Rev. B **40**, 3979 (1989).
[50]O. F. Sankey, D. J. Niklewski, D. A. Drabold, and J. D. Dow, Phys. Rev. B **41**, 12750 (1990).
[51]C. Freysoldt, B. Lange, J. Neugebauer, Q. Yan, J. L. Lyons, A. Janotti, and C. G. Van de Walle, Phys. Rev. B **93**, 165206 (2016).
[52]A. Resende, R. Jones, S. Öberg, and P. R. Briddon, Phys. Rev. Lett. **82**, 2111 (1999).
[53]J. P. Goss, M. J. Shaw, and P. R. Briddon, in *Theory of Defects in Semiconductors*, edited by D. A. Drabold and S. K. Estreicher (Springer, Berlin, 2007), p. 69.
[54]T. Prescha, T. Zundel, J. Weber, H. Prigge, and P. Gerlach, Mater. Sci. Eng. B **4**, 79 (1989).
[55]L. Dobaczewski, A. R. Peaker, and K. B. Nielsen, J. Appl. Phys. **96**, 4689 (2004).
[56]S. Dannefaer, P. Mascher, and D. Kerr, Phys. Rev. Lett. **56**, 2195 (1986).
[57]R. Kube, H. Bracht, E. Hüger, H. Schmidt, J. Lundsgaard Hansen, A. Nylandsted Larsen, J. W. Ager III, E. E. Haller, T. Geue, and J. Stahn, Phys. Rev. B **88**, 085206 (2013).
[58]T. Südkamp and H. Bracht, Phys. Rev. B **94**, 125208 (2016).
[59]S. K. Estreicher, Phys. Status Solidi B **217**, 513 (2000).
[60]N. Yarykin and J. Weber, Sol. State Phenom. **242**, 308 (2016).
[61]K. Sueoka, Y. Mukaiyama, K. Kobayashi, H. Fukuda, S. Yamaoka, S. Maeda, M. Iizuka, and V. M. Mamedov, ECS Trans. **86**, 3 (2018).
[62]O. V. Feklisova and N. Yarykin, Semicond. Sci. Technol. **12**, 742 (1997).
[63]N. Yarykin and J. Weber, Phys. Status Solidi A **216**, 1900304 (2019).
[64]M. Nakamura, S. Murakami, and H. Udono, Appl. Phys. Lett. **101**, 042113 (2012).